Tetrahedron Letters 49 (2008) 5196–5199

Contents lists available at ScienceDirect

Tetrahedron Letters

journal homepage: www.elsevier.com/locate/tetlet

Light-emitting persistent radicals for efficient sensor devices of solvent polarity

Marc López [a], Dolores Velasco [b,*], Francisco López-Calahorra [b], Luis Juliá [a,*]

[a] Departament de Química Orgànica Biològica, Institut d'Investgacions Químiques i Ambientals (CSIC), Jordi Girona 18-26, 08034 Barcelona, Spain
[b] Departament de Química Orgànica, Universitat de Barcelona, Martí i Franquès 1-11, 08028 Barcelona, Spain

ARTICLE INFO

Article history:
Received 19 May 2008
Revised 4 June 2008
Accepted 9 June 2008
Available online 12 June 2008

ABSTRACT

Radical adduct 1· and the novel [4-(*N*-indolyl)-2,6-dichlorophenyl] bis(2,4,6-trichlorophenyl)methyl radical (2·) exhibit intense fluorescence emission in cyclohexane in the red wavelength region. The intensity and the wavelength of the emission band are drastically dependent on the polarity of the solvent. Besides, radical adduct 2· has been fully characterized by differential scanning calorimeter, showing a high thermal stability and a clear glass nature to form excellent films.

Indole and carbazole derivatives display very interesting optical properties,[1,2] mainly those derivatives bearing an electron acceptor substituent in the nitrogen of the heterocycle.[3] These donor–acceptor compounds emit from charge-transfer excited states generated from the initially produced singlet excited states by charge transfer from the donor, indole, or carbazole, to the acceptor. A general feature of the emission spectra of these species is the dependence of the solvent polarity. In general, the spectra show a broadening of the emission line and a shift of the maximum to longer wavelengths with increased polarity of the solvent. In some cases, the solvent affects also the fluorescence quantum yield of the chromophore, decreasing the efficiency of the luminescence with increasing solvent polarity.

The luminescent properties of the carbazole derivatives prompted us to introduce a paramagnetic substituent in the heterocyclic molecule to study the influence of an open-shell moiety in the optical properties of the system. Therefore, a new adduct, (4-(*N*-carbazolyl)-2,6-dichlorophenyl)bis(2,4,6-trichlorophenyl)methyl radical (**1**·), by coupling the heterocyclic compound to tris(2,4,6-trichlorophenyl)methyl (TTM) radical, a very stable carbon-centered organic radical, was synthesized.[4] This paramagnetic adduct displays very attractive luminescent properties with emission efficiencies approximately as high as those of the parent carbazole and emission wavelengths dramatically shifted to the red region (for instance, $\lambda = 334/350$ nm for carbazole and $\lambda = 628$ nm for **1**· in cyclohexane). Recently, we have reported the preparation of a new series of radical adduct derivatives of **1**· by introducing electron-donor and acceptor substituents in the carbazole ring.[5] An analysis of the luminescent properties indicated a dramatic influence of solvent polarity on their emissions. As part of our research in new multifunctional species, here we report the synthesis of a new radical adduct, (4-(*N*-indolyl)-2,6-dichlorophenyl)bis(2,4,6-trichlorophenyl)methyl radical (**2**·), together with the absorption spectra and luminescent properties of **1**· and **2**· in different solvents. The electron paramagnetic resonance and the thermal properties of **2**·, studied by differential scanning calorimetry (DSC) and thermogravimetry (TGA), are also reported.

TTM radical in dimethylformamide at reflux (2 h) in Argon with an excess of indole and in the presence of cesium carbonate gave (4-*N*-indolyl-2,6-dichlorophenyl)bis(2,4,6-trichlorophenyl)methane (**2**),[6] which with an aqueous solution of tetrabutylammonium followed by oxidation with chloranil rendered pure radical adduct **2**·.[6] This paramagnetic species is a crystalline red solid, stable in solid state and in solution.

The TGA and DSC of **2**· are displayed in Figure 1. They exhibit a high and well-defined melting peak (260 °C) and an exothermic peak of decomposition at higher temperatures (DSC, onset temperature, 294 °C). The indole moiety of the adduct **2**· lowers considerably the melting temperature (~35 °C) relative to the carbazolyl adduct **1**·. Whereas **1**· melts with decomposition at higher temperature (295 °C),[3] **2**· is stable in the melting state moving away from the decomposition temperature and allowing to form amorphous glasses on cooling. Figure 2 shows a cyclic thermal diagram of **2**· with the temperature up to the melting temperature. A detailed analysis of the processes shows that on the first heating (10 °C min^{-1}) an exothermic polymorphic peak comes out at about 132 °C followed by a double thermal process, endo- and exothermic, at about 230 °C attributed most probably to a melting and recrystallization, and, finally, the well-defined melting at 260 °C. On cooling (10 °C min^{-1}), no reversible processes come out, forming a stable glass. The second heating (10 °C min^{-1}) shows a clear glass transition at about 95 °C which is not followed by a recrystallization.

X-band EPR spectra of the radical adduct **2**· recorded in CH_2Cl_2 solution (~10^{-3}–10^{-4} M) at 298 ± 3 K and 180 ± 5 K are shown in

* Corresponding authors. Tel.: +34 93 400 61 07; fax: 34 93 204 59 04 (L.J.).
E-mail address: ljbmoh@cid.csic.es (D. Velasco).

0040-4039/$ - see front matter © 2008 Elsevier Ltd. All rights reserved.
doi:10.1016/j.tetlet.2008.06.040

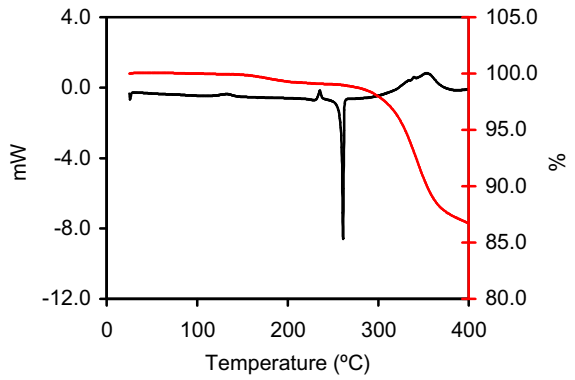

Figure 1. Thermal analysis of radical adduct **2**·. Dynamic diagram from 25.0 to 400 °C. Black: DSC analysis; red: TG diagram (heating rate 10.0 °C/min).

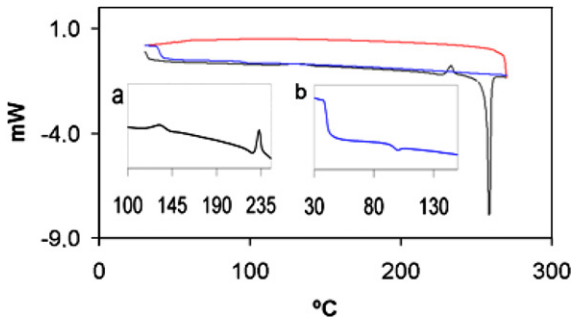

Figure 2. Thermal analysis results of radical adduct **2**· using DSC. Black: first heating; red: first cooling; blue: second heating. Inset: (a) detail for the first heating before melting; (b) detail for the second heating (heating and cooling rate: 10 °C/min).

Figure 3. The spectrum at room temperature consisted of a broad (peak to peak line width, ΔH_{pp} = 3.0 G) and single line with a Landé factor g = 2.0032 ± 0.0003, and a small equidistant pair of lines on both sides of the main spectrum appeared at higher values of the gain (Fig. 3, right). This small pair corresponds to the strong coupling (coupling constant, a(α-^{13}C) ~26.4 G) of the free electron with the α-^{13}C nucleus (natural abundance 1.11%). As the line width is mainly determined by a short spin–lattice relaxation time, τ_1, a decrease in the sample temperature has an important effect on the EPR spectrum, increasing τ_1 and reaching sufficiently narrow lines to make evident very small couplings which are not perceivable at room temperature. Thus, at low temperature (180 ± 5 K), the spectrum showed an overlapped multiplet of very close 7 lines (ΔH_{pp} = 0.75 G) corresponding to the weak coupling with six equivalent aromatic hydrogens in *meta*-positions (coupling constant value, a ~1.25 G), and two weak multiplets on both sides of the central multiplet attributed to the coupling with the three bridgehead-^{13}C nuclei adjacent to the α-carbon atom and with the six *ortho*-^{13}C nuclei (estimated coupling constant values by spectrum simulation,[7] a = 12.25 and 10.2 G, respectively) (Fig. 3, left).

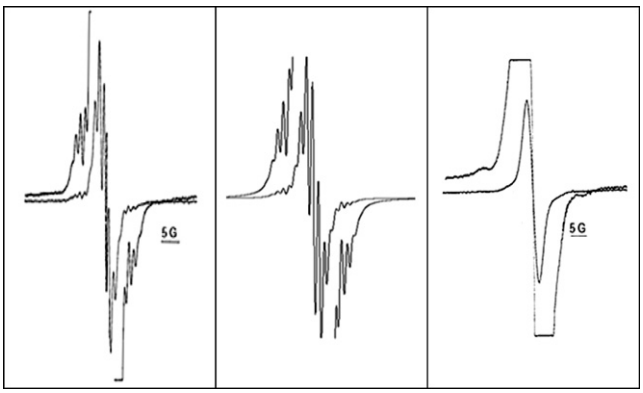

Figure 3. Left: EPR spectra of radical adduct **2**· in CH_2Cl_2 solution (~10^{-3} M) at 180 ± 5 K; modulation amplitude, 0.1. Center: Computer simulation.[7] Right: EPR spectrum of **2**· at rt.

The UV–vis absorption spectra of radical adduct **2**· in cyclohexane, chloroform, acetone, and ethanol are shown in Figure 4. The wavelengths and molar extinction coefficients of the maxima of radical adducts **1**· and **2**· in these solvents are displayed in Table 1. The UV–vis absorption values of the radical of reference, tris(2,4,6-trichlorophenyl)methyl (TTM) radical, in diluted $CHCl_3$ are as follows: $\lambda(\varepsilon)$, 373(38,100); 478(860); 542(834) nm. The structured lowest-lying band of **1**· and **2**· in $CHCl_3$ shows a remarkable red-shifted effect relative to that of TTM radical, confirming the large interaction between the carbazolyl and indolyl substituents and the triphenylmethyl radical moiety in the ground state. The absorption maxima do not change appreciably with solvent polarity. In fact, the only estimable difference is that the less energetic band is more structured in cyclohexane than in the other solvents. These two bands at λ = 373 ± 2 nm and 600 ± 3 nm are associated with the radical character of these species, corresponding the first one to a $\pi \rightarrow \pi^*$ transition due to the large associated molar absorptivities.

In contrast to the absorption spectra, the solvent polarity has a dramatic effect on the emission spectra of **1**· and **2**·. Values for the emission spectra in cyclohexane and chloroform are displayed in Table 2, and emission bands of radical adducts **1**· and **2**· in mixtures of cyclohexane and chloroform are shown in Figure 5. As shown in

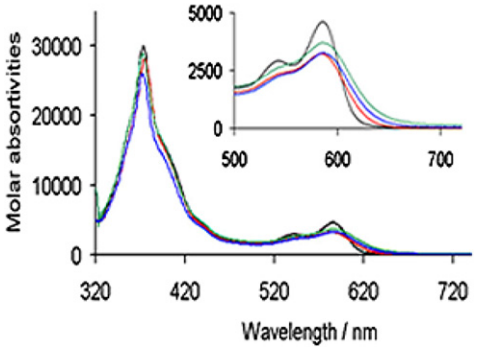

Figure 4. Absorption spectra of radical adduct **2**· in cyclohexane (black), $CHCl_3$ (red), and acetone (green) and ethanol (blue); the inset magnifies the lowest-lying band.

Table 1
Absorption data of **1**· and **2**· in cyclohexane, chloroform, acetone, and ethanol

	Cyclohexane $\lambda(\varepsilon^b)$ nm	Chloroform[a] $\lambda(\varepsilon^b)$ nm	Acetone $\lambda(\varepsilon^b)$ nm	Ethanol[c] $\lambda(\varepsilon^b)$ nm
1·	373(24,400) 554(sh)(2400) 603(4290)	374(25,600) 554(sh)(1990) 597(2940)	371(33,500) 552(sh)(2400) 597(3460)	
2·	373(30,000) 542(sh)(2920) 585(4620)	375(28,200) 542(sh)(2340) 584(3230)	373(28,900) 542(sh)(2620) 586(3700)	372(26,000) 542(sh)(2250) 586(3260)

[a] Values for radical adduct **1**· are taken from Ref. 3.
[b] Units: $dm^3\ mol^{-1}\ cm^{-1}$.
[c] Radical adduct **1**· is not soluble in ethanol.

the figure, the emission bands of both radical adducts shift to the red, broaden, and decrease in intensity with increasing solvent polarity. The red-shift is more pronounced in **1**· than in **2**·. The fact that only the emission and not the absorption is affected by change of solvent polarity indicates the existence of a strong interaction of the solvent with the excited state and not with the ground state of the molecule and, consequently, the different nature of both electronic states. In cyclohexane solution, both radical adducts exhibit also a weak extra emission band overlapped with the main band at the longer wavelength side of the spectra (Fig. 6). This extra weak band may be attributed to emission from a twisted intramolecular charge-transfer (TICT) excited state, similarly as it has been reported in the literature for many other donor–acceptor luminescents.[3] The radical adducts **1**· and **2**· are compounds with the carbazolyl and indolyl moieties as electron donors linked by a single bond with a good electron-acceptor moiety (the triphenylmethyl radical). In summary, excitation of **1**· and **2**· takes place from a ground doublet state to a low-lying neutral excited state, also doublet in character, and the emission from a charge-transfer excited state. The excited state is additionally stabilized by the polarity of the solvent to a lowest-energy twisted conformation. This is why in the emission spectra of **1**· and **2**· in $CHCl_3$ appear only as the less energetic band. The charge-transfer character of the excited state is corroborated by the large Stokes values found in chloroform (Table 2).

Both radical adducts **1**· and **2**· do not exhibit any emission in acetone, and **2**· neither in ethanol (**1**· is not soluble in ethanol). The emission bands of **1**· and **2**· in cyclohexane are red-shifted and drastically decreased in the presence of very low concentrations of acetone or ethanol. In Figure 7, the quenching values of the emission of **1**· and **2**· in cyclohexane as a function of the concentration of acetone and ethanol are displayed. Excitation of electron donor–acceptor molecules to an excited state in a polar medium, followed by a rapid relaxation to a charge-transfer state far from the Franck–Condon configuration, induces a large reorientation of the surrounding solvent molecules. In these conditions, the nonradiative dissipation of the electronic energy can easily compete with the radiation decay. When the quenching of fluorescence is due to ethanol, the radiationless deactivations might be induced by intermolecular hydrogen bond between the O–H of ethanol and the nitrogen of the carbazole moiety. These effects are much more moderate with chloroform as the quenching agent.

A new stable radical adduct **2**· of the TTM series has been prepared from the reaction of TTM radical and indole. The optical response of **2**· as well as that of the radical adduct of TTM radical with carbazole, **1**·, in solution is a clear example of the effect of solvent on the quenching of fluorescence. The emission wavelength and the quantum yield are drastically dependent on the nature of the molecular environment around the fluorophore. These drastic effects suggest that both paramagnetic species might be used as solvent polarity sensors. On the other hand, the high thermal stability, excellent film forming property, and good solubility in halogenated organic solvents of **2**· are potentially useful for applications as component of light-emitting diodes. The electrochemical behavior, the electron and hole conductivities, and the susceptibility measurements of **2**· are being studied in our laboratories.

Table 2
UV–vis and luminescence spectral data[a] for **1**· and **2**· in cyclohexane and chloroform

		λ_{abs}[a,b]	λ_{exc}[a]	λ_{em}[a]	Φ_F[c]	Stokes shift[d]
1·	Cyclohexane	603	515	628	0.53	660
	Chloroform	597	515	687	0.02	2257
2·	Cyclohexane	585	450	610	0.52	700
	Chloroform	584	450	646	0.003	1643

[a] Values of λ in nm.
[b] The less energetic band in the absorption spectra.
[c] Quantum yield of luminescence.
[d] Values in cm^{-1}.

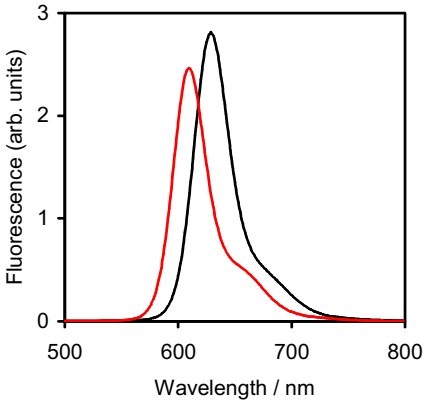

Figure 6. Luminescence spectra of radical **1**· (black) and radical **2**· (red) in cyclohexane.

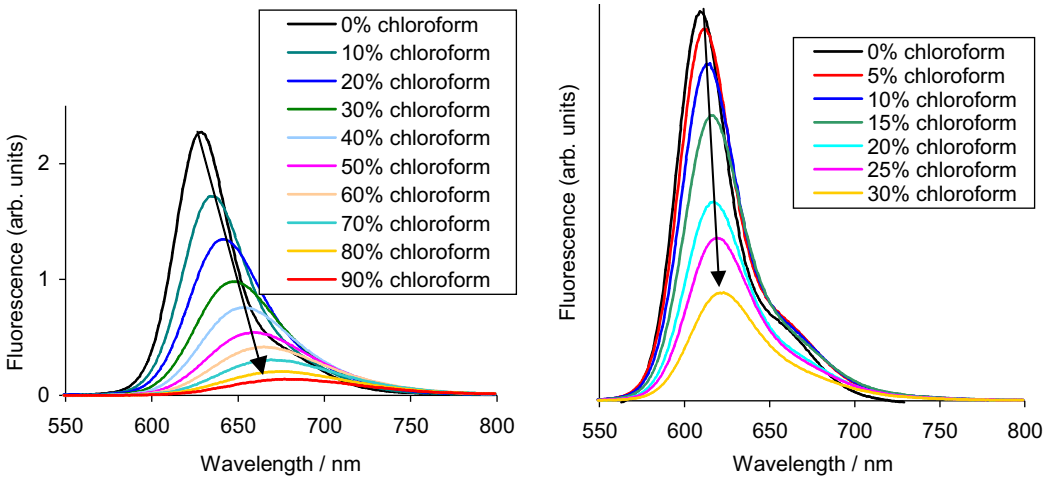

Figure 5. Emission spectra of radical **1**· (left) and radical **2**· (right) in different solvent polarities (cyclohexane/chloroform, v/v) (excitation light, 450 nm).

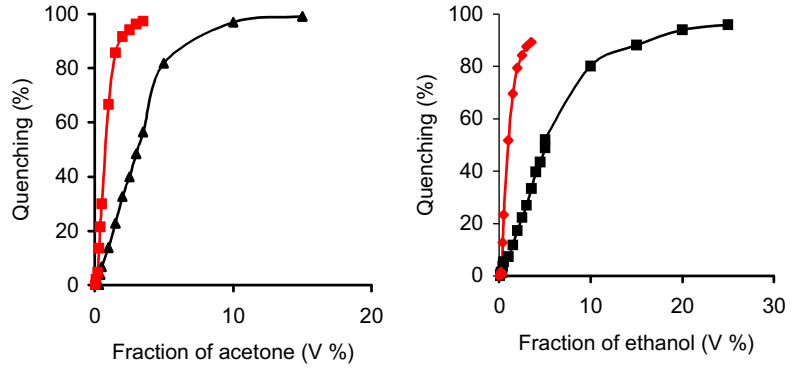

Figure 7. (Left): Quenching values of emission of **1**· (black) and **2**· (red) versus acetone fraction in cyclohexane (acetone/cyclohexane, v/v). (Right): Quenching values of emission of **1**· (black) and **2**· (red) versus ethanol fraction in cyclohexane (ethanol/cyclohexane, v/v).

Acknowledgments

Financial support for this work from the MEC (Spain) through project CTQ2006-15611-C02-02/BQU is gratefully acknowledged. We also thank the EPR service of the Centre d'Investigació I Desenvolupament (CSIC) for recording the spectra.

References and notes

1. References on carbazole, see: Favini, G.; Gamba, A.; Grasso, D.; Millefio, S. *Trans. Faraday Soc.* **1971**, *67*, 3139–3143; Schneide, F.; Zander, M. *Ber. Bunsen-Ges. Phys. Chem.* **1971**, *75*, 887–892; Iwashima, S.; Kuramachi, M.; Aoki, J. *Nippon Kagaku Kaishi* **1976**, 858–864; Dreger, Z.; Kalinowski, J.; Nowak, R.; Sworakowski, J. *Chem. Phys.* **1988**, *126*, 417–424; Bisht, P. B.; Tripathi, H. B. *J. Lumin.* **1993**, *55*, 153–158; Mo, Y. M.; Bai, F. L.; Wang, Z. T. *J. Photochem. Photobiol. A* **1995**, *92*, 25–27; Grazulevicius, J. V.; Soutar, I.; Swanson, L. *Macromolecules* **1998**, *31*, 4820–4827; Sarkar, A.; Chakravorti, S. *J. Lumin.* **1998**, *78*, 205–211; De, A. K.; Ganguly, T. *J. Lumin.* **2001**, *92*, 255–270; Chen, L. X.; Niu, C. G.; Zeng, G. M.; Huang, G. H.; Shen, G. L.; Yu, R. Q. *Anal. Sci.* **2003**, *19*, 295–298; Belletete, M.; Bedard, M.; Leclerc, M.; Durocher, G. *Synth. Met.* **2004**, *146*, 99–108; Romero-Ale, E. E.; Olives, A. I.; Martin, M. A.; del Castillo, B.; Lopez-Alvarado, P.; Menendez, J. C. *Luminescence* **2005**, *20*, 162–169; Wang, W.; Fang, Q.; Lui, Z. Q.; Cao, D. X.; Deng, M. Z. *Acta Chim. Sinica* **2005**, *63*, 1323–1328; Shao, H. X.; Chen, X. P.; Wang, Z. X.; Lu, P. *J. Lumin.* **2007**, *127*, 349–354.
2. Referentes on indole, see: Balemans, M. G.; Vandevee, F. c. *Experientia* **1967**, *23*, 906; Delauder, W. B.; Wahl, P. *Biochim. Biophys. Acta* **1971**, *243*, 153; Tatischeff, I.; Klein, R. *Photochem. Photobiol.* **1975**, *22*, 221–229; Ricci, R. W.; Nesta, J. M. *J. Phys. Chem.* **1976**, *80*, 974–980; Pandya, M. L.; Machwe, M. K. *J. Chem. Phys.* **1978**, *68*, 341–342; Klein, R.; Tatischeff, I.; Bazin, M.; Santus, R. *J. Phys. Chem.* **1981**, *85*, 670–677; Aaron, J. J.; Tine, A.; Villiers, C.; Parkanyi, C.; Bouin, D. *Croat. Chem. Acta* **1983**, *56*, 157–168; Fucaloro, A. F.; Forster, L. S.; Campbell, M. K. *Photochem. Photobiol.* **1984**, *39*, 503–506; Escudero, J. L.; Montoro, T.; Campillo, A. L. *J. Lumin.* **1985**, *33*, 435–446; Martinez, E.; Escudero, J. L.; Campillo, A. L. *J. Mol. Struct.* **1986**, *143*, 317–320; Krishnamurthy, M.; Mishra, A. K.; Dogra, S. K. *Photochem. Photobiol.* **1987**, *45*, 359–364; Arena, A.; Martino, G.; Mezzasalma, A. M.; Mondio, G.; Saitta, G. *J. Lumin.* **1991**, *48–9*, 363–367; Medina, F.; Poyato, J. M. L.; Pardo, A.; Rodriguez, J. G. *J. Photochem. Photobiol. A* **1992**, *67*, 301–310; Vincent, M.; Gallay, J.; Demchenko, A. P. *J. Phys. Chem.* **1995**, *99*, 14931–14941; Sulkes, M.; Borthwick, I. *Chem. Phys. Lett.* **1997**, *279*, 315–318; Singh, A. K.; Hota, P. K. *Res. Chem. Intermediat.* **2005**, *31*, 85–101.
3. Van Duuren, B. L. *Chem. Rev.* **1963**, *63*, 325–354; Grabowski, Z. R.; Rotkiewicz, K.; Rettig, W. *Chem. Rev.* **2003**, *103*, 3899–4031 and references cited therein.
4. Gamero, V.; Velasco, D.; Latorre, S.; López-Calahorra, F.; Brillas, E.; Juliá, L. *Tetrahedron Lett.* **2006**, *47*, 2305–2309.
5. Velasco, D.; Castellanos, S.; López, M.; López-Calahorra, F.; Brillas, E.; Juliá, L. *J. Org. Chem.* **2007**, *72*, 7523–7532; Castellanos, S.; Velasco, D.; López-Calahorra, F.; Brillas, E.; Juliá, L. *J. Org. Chem.* **2008**, *73*, 3759–3767.
6. *Selected data* for **2** and **2**·. Compound **2**: IR (KBr) 3070(w), 1598(s), 1579 (m), 1545 (s), 1476 (s), 1468 (s), 1449 (w), 1372 (m), 1332(m), 1296 (w), 1259 (w), 1236 (w), 1211 (m), 1193 (w), 1175 (m), 1136 (m), 1023 (m), 899 (m), 859 (s), 837 (w), 804 (s), 761 (m), 742 (s), 714 (w), 677 (w) cm^{-1}; ^1H NMR (300 MHz, $CDCl_3$) δ 7.64 (d, 1H, J = 7.8 Hz), 7.57 (d, 1H, J = 7.8 Hz), 7.51 (d, 1H, J = 2.4 Hz), 7.37 (d, 1H, J = 2.4 Hz), 7.36 (d, 1H, J = 3.3 Hz), 7.35 (d, 1H, J = 3.3 Hz), 7.29 (d, 1H, J = 3.3 Hz), 7.24–7.14 (m, 4H), 6.75 (s, 1H), 6.67 (dd, 1H, J = 3.3 Hz, J' = 0.9 Hz). MS (MALDI-TOF): m/z = 633.3 (M^+-1). Anal. Calcd for $C_{27}H_{13}Cl_8N$: $CHCl_3$ (8:3) C, 48.4; H, 2.0; N, 2.1. Found: C, 48.7; H, 2.1. Compound **2**·: IR (KBr) 3070 (w), 1577 (s), 1554 (m), 1525 (s), 1474 (m), 1464 (s), 1370 (m), 1332 (m), 1297 (w), 1235 (w), 1210 (m), 1183 (m), 1134 (m), 1082 (w), 924 (w), 858 (m), 812 (m), 799 (m), 764 (w), 740 (m), 716 (w) cm^{-1}; MS (MALDI-TOF): m/z = 634.4 (M^++1). Anal. Calcd for $C_{27}H_{12}Cl_8N$: $CHCl_3$ (8:1) C, 50.2; H, 1.9; N, 2.2. Found: C, 50.3; H, 1.9; N, 2.0.
7. WINSIM program provided by D. Dulog, Public EPR Software Tools, National Institute of Environmental Health Sciences, Bethesda, MD, 1996.